



Uplift Resistance of Buried Pipelines and DNV-RP-F110 Guidelines

N.I Thusyanthan¹, S. Mesmar¹
J. Wang² & S.K. Haigh²

¹KW Ltd., Fetcham Park House, Fetcham, Surrey, U.K

²Engineering Department, University of Cambridge, U.K

1. Introduction

Offshore pipelines are commonly buried in the seabed. The purpose of burying subsea pipelines is three-fold. Firstly, the soil cover protects the pipeline from damage due to trawlers or anchors. Secondly, the overlying soil provides thermal insulation to maintain temperature that can be necessary for the satisfactory flow of the oil or gas. Lastly, the burial resists the upward bending of the pipeline due to expansion, caused by thermal stresses, which might eventually lead to structural failure. This phenomenon is known as upheaval buckling.

Upheaval buckling is a common design issue for buried pipelines when the out-of-straightness of the pipeline, and the high axial compressive forces induced due to the extreme operating conditions, causes the pipeline to buckle upwards (Figure 1). In order to prevent upheaval buckling, the pipeline has to be buried deep enough such that the soil cover is sufficient in providing adequate uplift resistance. The required upward movement, or mobilisation, of the pipeline to achieve the desired uplift resistance is a vital design parameter, in that pipeline integrity under operating conditions relies upon its value.

Research results over the last two decades have provided better understanding and insight into the failure mechanisms associated with upheaval behaviour of pipelines such that we are able to correctly predict the peak uplift resistance provide by soil cover. However, the majority of the results have been from either small scale lab testing or centrifuge testing. Hence, one of the key design parameters, the mobilisation distance (Figure 6), is still not fully understood. The current design practice DNV-RP-F110 on uplift resistance prediction is based on a tri-linear design curve. This guideline suggests that the maximum uplift resistance in sandy backfill is mobilised when the upward movement of the pipe reaches 0.5%H to 0.8%H, where H is the cover height defined as the vertical distance from top of pipe.

This paper presents a comprehensive summary of all the available uplift test data in literature along with new full scale uplift test data conducted at the Schofield Centre, University of Cambridge, in sandy backfill. The results show that the mobilisation distance to peak uplift resistance depends on the ratio of soil cover to pipe diameter and it exceeds the DNV RP-F110 recommended values. A new equation for mobilisation distance as a function of H/D is proposed.

Figure 1 shows a typical cross sectional view of upheaval buckling of a buried offshore pipeline.

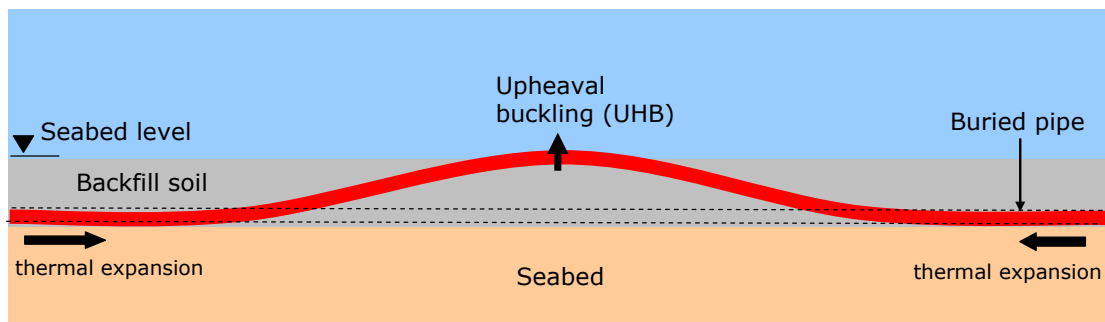


Figure 1 Upheaval buckling of a buried pipeline

2. Review of Literature

The structural aspects of the UHB problem are well understood. The UHB stability of the pipeline is governed by force balance between the axial compressive force P and the available downward restraints (Timoshenko and Goodier, 1934). 4th order general solution is of the form (Palmer et al., 1990):

$$\phi_w = A \left(\frac{\pi}{\phi_L} \right)^2 - B \left(\frac{\pi}{\phi_L} \right)^4 \quad \text{Eq. (1)}$$

where $\phi_w = \frac{wEI}{\delta P^2}$ is the dimensionless uplift resistance; $\phi_L = L \sqrt{\frac{P}{EI}}$ is the dimensionless imperfection length; w is the download per unit length; EI is the flexural rigidity of the pipeline; P is the thermally-generated axial compressive force; δ is the maximum height of the imperfection; L is half the total imperfection length; And A , B are constants to be determined numerically. The solution for any particular pipeline section will depend on the initial imperfection profile (Croll, 1997). As ϕ_w intrinsically depends upon δ , any additional upward movement of the pipeline would act as feedback into calculation. Hence the exact equilibrium

is also related to how the available uplift resistance is mobilised as the pipeline moves upwards through the soil cover.

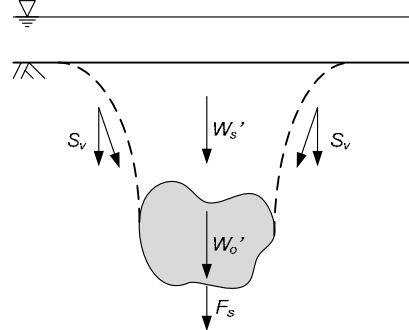


Figure 2 Components of uplift resistance for an object buried in seabed

The initial breakout resistance of objects embedded underground consists of four components¹ (Versic, 1971), as illustrated in Figure 2:

1. The submerged effective weight of the object, W'_o
2. The submerged effective weight of soil being lifted, W'_s
3. The vertical component of the soil shearing resistance, S_v
4. The vertical component of the suction force due to excess pore pressure differences above and below the object, F_s

For pipeline upheaval buckling (UHB) design, the W'_o term can be accurately assessed and is independent of cover conditions. The contribution from F_s depends directly on the pull-out speed (Bransby and Ireland, 2009, and Wang et al., 2009, Thusyanthan et al., 2008), hence it is sufficient and conservative to assume fully drained scenarios. Therefore, the contribution from the cover soil is the sum of W'_s and S_v only. This “true” uplift resistance depends on the deformation mechanism as well as properties of the soil.

In cohesionless soils, one popular hypothetical mechanism is the “Vertical Slip Surface” model with linearly varying shear resistance with increased depth, as illustrated in Figure 3(a). The peak “true” uplift resistance per unit length, R_{peak} , can be derived from equilibrium in the vertical direction (Pederson and Jensen, 1988):

$$\frac{R_{peak}}{\gamma'HD} = 1 + 0.1 \frac{D}{H} + f_p \left[\frac{D}{H} \times \left(\frac{H}{D} + \frac{1}{2} \right)^2 \right] \quad \text{Eq. (2)}$$

where f_p is the dimensionless Pederson Uplift Factor. This is the DNV RP F110 recommended form for the prediction of uplift resistance. It is to be noted that a

¹ Versic, (1971) includes a fifth component as the adhesion between the object and the adjacent soil. Schofield and Wroth, (1968) suggests that adhesion arises from negative pore water pressures during soil dilation, hence is indistinguishable from F_s .

simplified expression can be obtained by using only the soil above the top of the pipe (Schaminée et al., 1990), this gives:

$$\frac{R_{peak}}{\gamma'HD} = 1 + f_s \frac{H}{D} \quad \text{Eq. (3)}$$

where f_s is the Schaminée uplift resistance factor for cohesionless soils. It is important to distinguish the Pederson and Schaminée uplift factors.

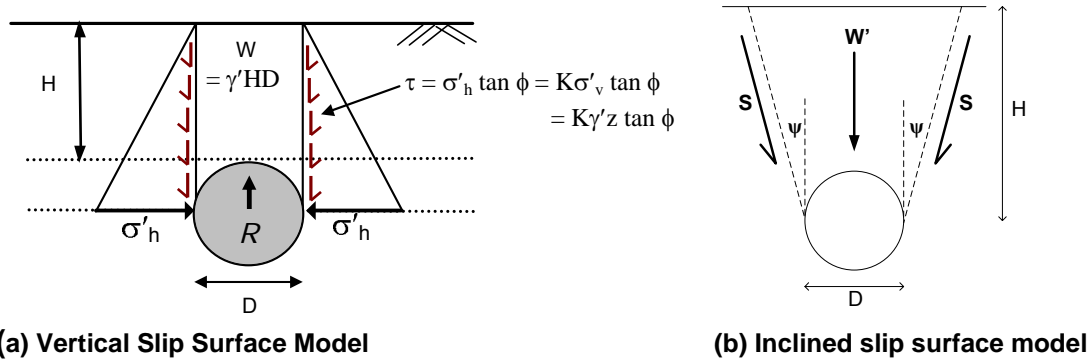


Figure 3 Uplift Models

For UHB in medium to dense sandy backfill, the Inclined Slip Surface Model (Figure 3(b)), which employs the dilatancy of the soil, is experimentally proven (White et al, 2001) to be a closer approximation to the real deformation mechanism. By assuming that the normal effective stress, σ_n' , remains constant during the uplift event, the normalised uplift resistance according to this model can be expressed as²:

$$\frac{R_{peak}}{\gamma'HD} = 1 + 0.1 \frac{D}{H} + \left\{ \tan \psi + \frac{1}{2} (\tan \phi_{peak} - \tan \psi) [1 + K_0 - (1 - K_0) \cos 2\psi] \right\} \times \left[\frac{D}{H} \times \left(\frac{H}{D} + \frac{1}{2} \right)^2 \right] \quad \text{Eq. (4)}$$

The design equation from the inclined slip-surface model and the vertical slip surface model are algebraically indistinguishable, and identifying a suitable f_p value from model tests will be sufficient for design purposes.

Experiment-based uplift resistance analyses have become plentiful over the past two decades (Dickin 1994, Baumgard 2000, White et al. 2001, Palmer et al. 2003, Dickin and Laman 2007, Check et al. 2008). However, test data from Trautmann et al. (1985) remain the most influential in current design process as DNV RP F110 seems to be based on its results. Trautmann et al. (1985) carried out a series of full-scale uplift resistance tests in Washed-and-oven-dried Cornell filter sand ($D_{10} = 0.2$ mm). Three backfill bulk densities were tested: 14.8 kN/m^3

² The equation from the original paper has been modified to adopt a consistent definition for H, being the distance between the soil surface and the pipe crown

(loose), 16.4 kN/m^3 (medium), and 17.7 kN/m^3 (dense). It should be noted that the medium and dense densities were achieved via compaction at 100 mm intervals. Therefore data from these tests are not directly applicable for offshore design. The pullout rate was 20 mm/min, which corresponds to approximately three sand grains per second. The recorded normalized uplift force-displacement curves have been reproduced in Figure 4. Significant scatter and noise are evident. Mobilisation in loose sand seems to be smaller than in medium dense (compacted) sand which is unexpected. The large alternating peaks and troughs for $H/D = 13$ in loose sand should not have occurred given the large cover height. Regarding mobilization, the original paper acknowledged problems with the displacement measuring system. Hence, the reliability of the initial displacement data is questionable, especially as mobilisation in loose sand seems to be smaller than in medium sand.

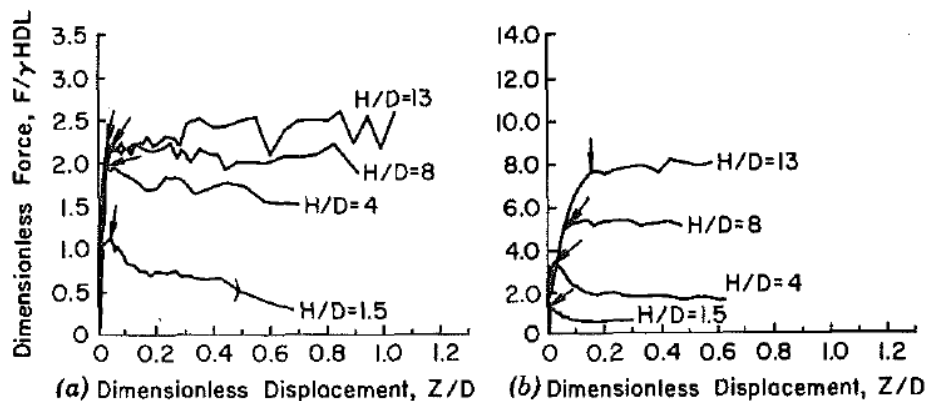


Figure 4 Load-displacement data from Trautmann et al., (1985) (a) loose sand (b) medium dense sand (compacted)

3. DNV RP F110 Guidelines

The DNV RP F110 is the recommended practice for “global buckling of submarine pipelines”. This is a common industry standard that is being used for design of upheaval buckling of buried pipelines. The guideline addresses the issue of buckling in three different sections depending of the pipeline state as below,

- Pipelines exposed on even seabed
- Pipelines exposed on un-even seabed
- Buried Pipelines

Under each case the guideline provides steps for buckling design and possible mitigation measures as shown in Figure 5. This paper concentrates on the issue of “Soil Resistance Modelling” applicable for buried pipelines.

Appendix B of the code provides guidance on the soil uplift resistance modelling. It also recommends the use for tri-linear resistance model to represent the uplift resistance of cohesionless soil. The recommended tri-linear soil resistance curve (range) is shown in Figure 6(a). The recommended curve is based on the normalised displacement where the δ_f is the peak mobilisation distance and α and β values determine the middle point in the tri-linear curve. Uplift parameters provided in DNV RP F110 are summarised in Table 1. For loose sand, α value of 0.75-0.85 and β of 0.2 is provided.

Pipeline exposed on even seabed -governing deformation takes place in the horizontal plane	Pipeline exposed on uneven seabed -deformation initially occurs in the vertical plane and subsequently in the horizontal plane	Buried Pipeline -pre-installed phase -as installed phase
Step 1 Global Buckling (Pre-buckling) Step 2 Pipe Integrity Check Step 3 Mitigation measures	Step 1 Global Buckling (Pre-buckling) Step 2 Pipe Integrity Check Step 3 Mitigation measure checks	Step 1 Specific Cover design Soil Resistance Modelling Step 2 Minimum cover design Step 3 Specification of Cover Step 4 Pipe Integrity Check

Figure 5 Summary of DNV RP F110

For FE modelling of the soil resistance, the guideline states that the uplift resistance be reduced with a safety factor γ_{UR} . Thus the normalised tri-linear uplift resistance model would be as shown in Figure 6(b). The value of γ_{UR} depends on the soil type as given below.

$$\gamma_{UR} = 0.85 + 3 \cdot \sigma_{configuration} \quad \text{Non-cohesive soil (Sand and Rock)}$$

$$\gamma_{UR} = 1.1 + 3 \cdot \sigma_{configuration} \quad \text{Cohesive soil (Clay)}$$

where $\sigma_{configuration}$ is the standard deviation for the survey accuracy of the pipeline configuration. The code states that the minimum value to be used for $\sigma_{configuration}$ as 0.025 m. However, this minimum value would lead to $\gamma_{UR} = 0.925$ for cohesionless backfill. For simplicity, the value of γ_{UR} is considered as unity in this paper.

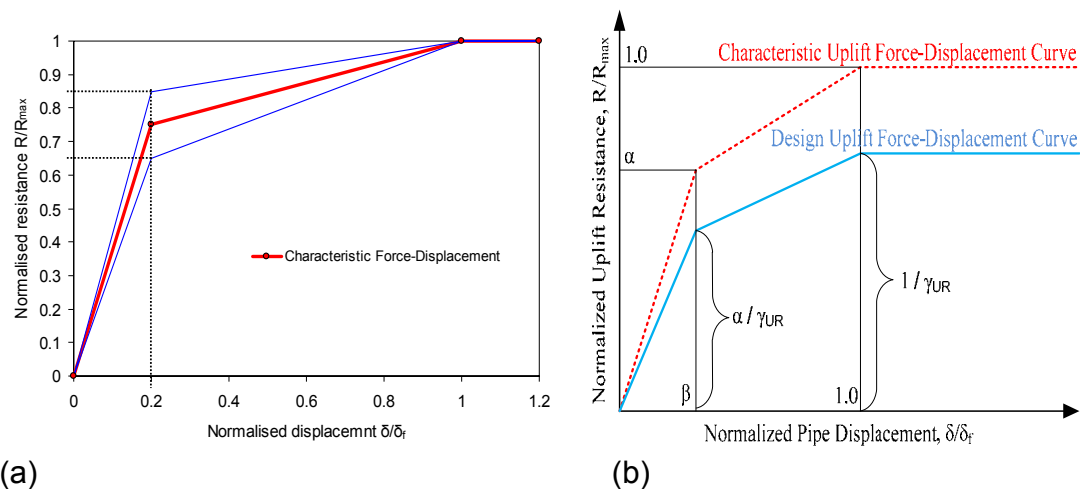


Figure 6 Normalised Uplift Resistance recommended in DNV RP F110

Backfill soil	Type	γ' (kN/m ³)	Mobilisation distance δ_f	α	β	Pedersen uplift factor f	Limitation
SANDs Cohesionless Soil	Loose	8.5	0.5%-0.8%H*	0.75-0.85	0.2	0.1-0.3	$3.5 \leq H/D \leq 7.5$
	Medium /Dense	9-10	0.5%-0.8%H*	0.65-0.75	0.2	0.4-0.6	$2 \leq H/D \leq 8$
CLAYs Cohesive Soil	Jetting	4-8	0.03D-0.07D	0.5	0.2	-	$1 < H/D < 8$
	Ploughing	5.5-8.5	0.2D-0.4D	0.5	0.2	0.25-0.40	$1 < H/D < 8$
	Local soil failure	DNV (in house) experience from full Scale tests in remoulded material suggests that the maximum resistance offered by a local soil failure in soft clay will required mobilisation $\delta_f / D = 1-3\%$. In fluidised clay the mobilisation values can be in excess of $\delta_f / D = 15\%$					
	Global soil failure	The test that are carried out (DNV) have shown δ_f / H ratios of <ul style="list-style-type: none"> 7-8% for remoulded clay 1-6% for intact clay and 20-40%for intact clay lumps 					
Rock	-	-	20-30 mm (based on limited tests)	0.7	0.2	0.5-0.8	$2 \leq H/D \leq 8$, Particle size (25 mm – 75 mm)

Note * δ_f is given as 0.005-0.01H in the text of DNV RP F110 in pg 44.

Table 1 Summary of DNV RP F110 Uplift Parameters

4. Full Scale Testing

4.1. Test setup

In order to understand the mobilisation distance in cohesionless soils, a series of full scale uplift tests were carried out at the Schofield Centre, University of Cambridge. The test series, shown in Table 2, can be divided into two categories:

1. Plane-strain testing in saturated (submerged) sand (Tests 1-8)
2. Full scale testing in moist sand (Tests 9 & 10)

Figure 7 shows a schematic plot and a photograph of the plane-strain test tank. The tank can be dissembled into two components: the bottom container and the top actuator. The bottom container has internal dimensions of 1000 mm (L) × 76 mm (W) × 850 mm (H). It has a steel framework, base and back to provide adequate strength in heavy-duty experiments. Its front face features a transparent Perspex cover, detachable from the frame. This enables direct observation of backfill movement and, more importantly, the possibility of using Particle Image Velocimetry (PIV), (White et al.2003) technique to reveal the displacement field of the backfill throughout the pull-out event. Two additional pieces of laminated glass are fitted to the internal front and back faces of the container. A 7 × 7 grid of control markers is drawn on the front glass piece for PIV calibration.

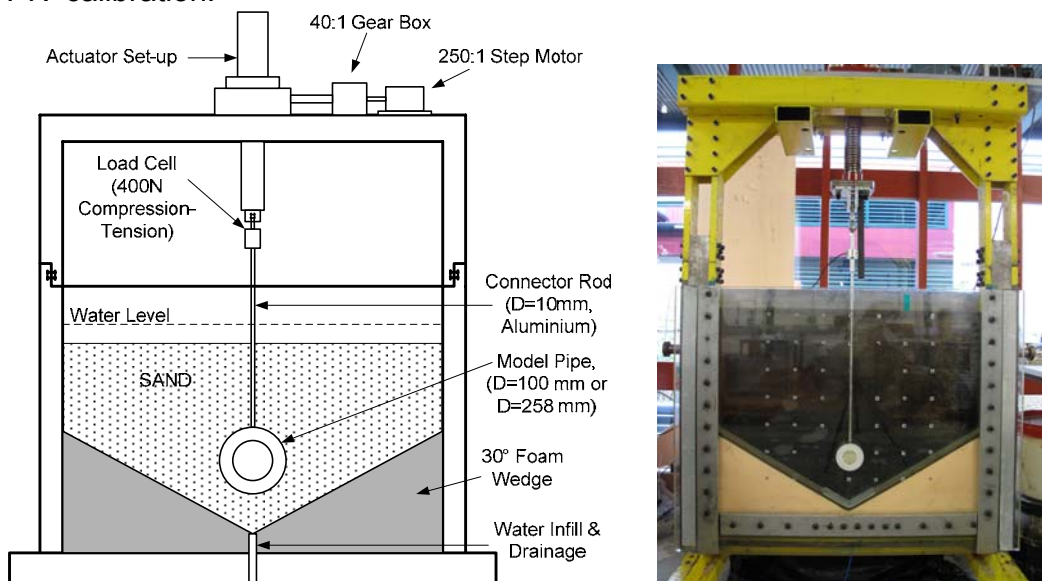


Figure 7 Experimental Test Setup

Two model pipes of external diameters 100 mm and 258 mm with PTFE front and back ends were used in the tests. The PTFE material has negligible friction angle against glass, which minimises the end effects in 2D plain strain modelling. Both pipes were connected to the upper actuator via a 10 mm diameter

aluminium rod. The cross sectional area of the rod represents 1.03% of the projected area of the 100 mm diameter model pipe and 0.40% of the 258 mm diameter model pipe, thus its effect on the measured uplift resistance can be regarded as negligible.

Fraction E sand of relative density $I_D = 35\%$ (loose), median diameter D_{50} of 0.18 mm (Figure 8) and saturated unit weight γ_{sat} of 18.5 kN/m^3 was used as backfill. Critical friction angle of the sand is 32° . All tests in the plane strain test tank were carried out under fully submerged conditions.

Tests No. 9 and 10 were conducted in full scale tank (2250 mm width \times 2000mm height) using fine sand with all properties very similar to that of Fraction E Sand. The tests were done unsaturated and at in-situ moisture content (approximately 5%). The bulk unit weight of the sand was approximately 15 kN/m^3 in both tests. The model pipe used has external diameter of 0.2 m. Further tests were also carried out to confirm the repeatability of the tests. These are not reported in this paper.

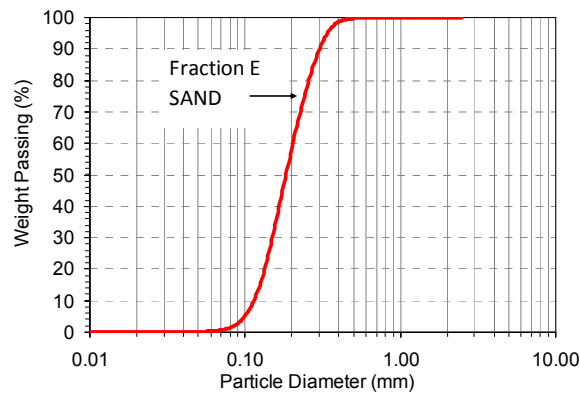


Figure 8 Particle size distribution of SAND, gravel

Test No.	Backfill	H/D	Pipe Diameter (mm)	Measured δ_f (mm)	DNV $\delta_f(0.01H)$ mm	R_{peak}	f_p
1	Sand (submerged)	0.1	100	2.5	0.10	0.052	1.09
2	Sand (submerged)	0.4	100	3	0.40	0.115	1.01
3	Sand (submerged)	0.5	100	2.5	0.50	0.130	0.89
4	Sand (submerged)	1	100	3.3	1.00	0.270	0.89
5	Sand (submerged)	2	100	4.6	2.00	0.50	0.58
6	Sand (submerged)	3.5	100	10	3.50	1.24	0.68
7	Sand (submerged)	0.5	258	10	1.29	0.6	0.43
8	Sand (submerged)	1.0	258	8	2.58	1.4	0.58
9	Sand (moist)	6	200	110	12.00	18.3	0.56
10	Sand (moist)	8	200	215	16.00	24.2	0.43

Table 2 Summary of Tests and Results

4.2. PIV Analysis of digital pictures

The principles of PIV analysis (White et al., 2003) is summarised in Figure 9. PIV operates by tracking the texture (i.e. the spatial variation of colour and brightness) within an image of soil through a series of images. The initial image is divided up into a mesh of PIV patches. Consider one of these patches, located at coordinates (u_1, v_1) in image 1 (Figure 9). To find the displaced location of this patch in a subsequent image, the following operation is carried out. The correlation between the patch extracted from image 1 (time = t_1) and a larger search patch (zone) from the same part of image 2 (time = t_2) is evaluated. The location at which the highest correlation is found indicates the displaced position of the patch (u_2, v_2). This operation is repeated for each of the mesh of patches within the image, and then repeated for each image within the series to produce complete trajectories of each patch movement.

As further illustration, the PIV mesh for Test No. 5 is shown in Figure 10.

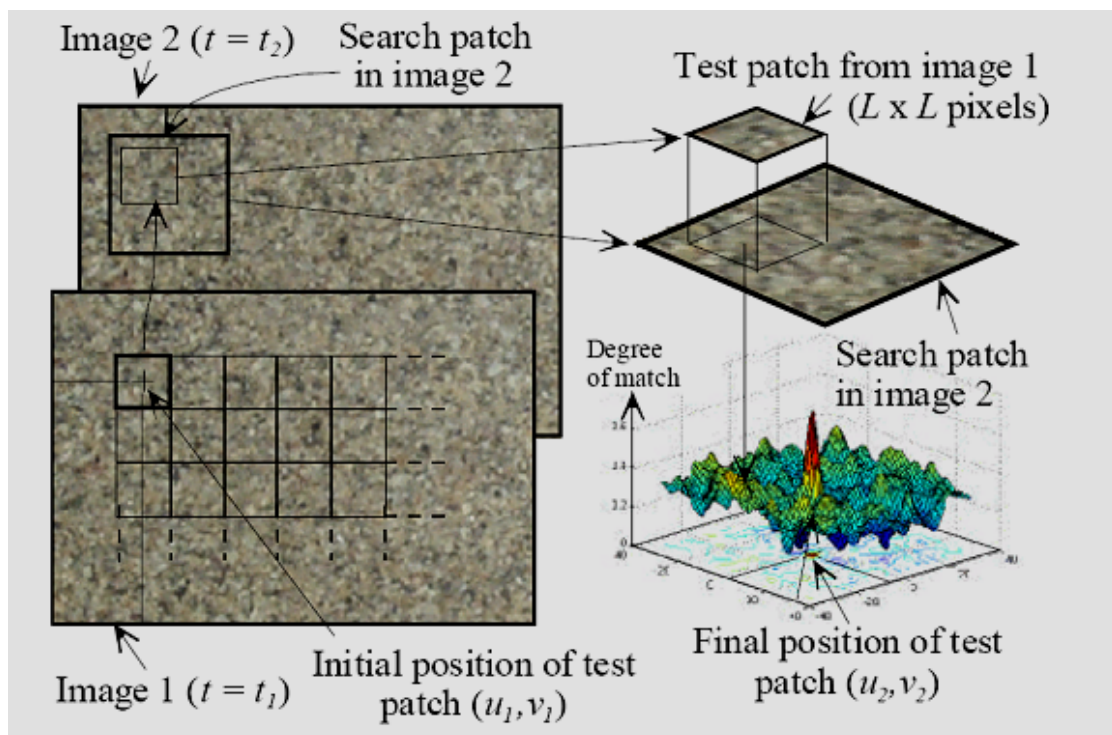


Figure 9 Principles of PIV analysis

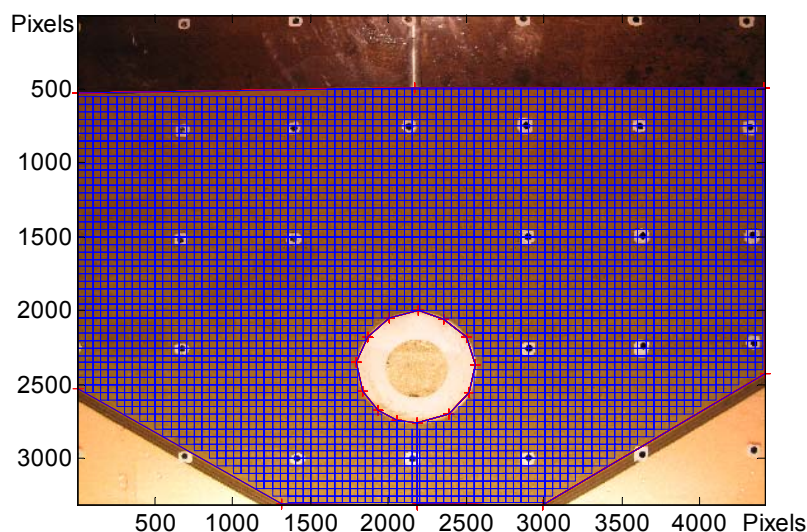


Figure 10 PIV patches (50×50 pixel used in Test No. 5 ($H/D = 2$, $D=100$ mm))

5. Results

A summary of test results are presented in Table 2.

5.1. Mobilisation Distance

Test results from series 1 and 2 ($D=200$ mm) are Figure 11 and Figure 12 respectively. It is clear from Table 2 that the mobilisation is much higher than DNV guideline as H/D increases.

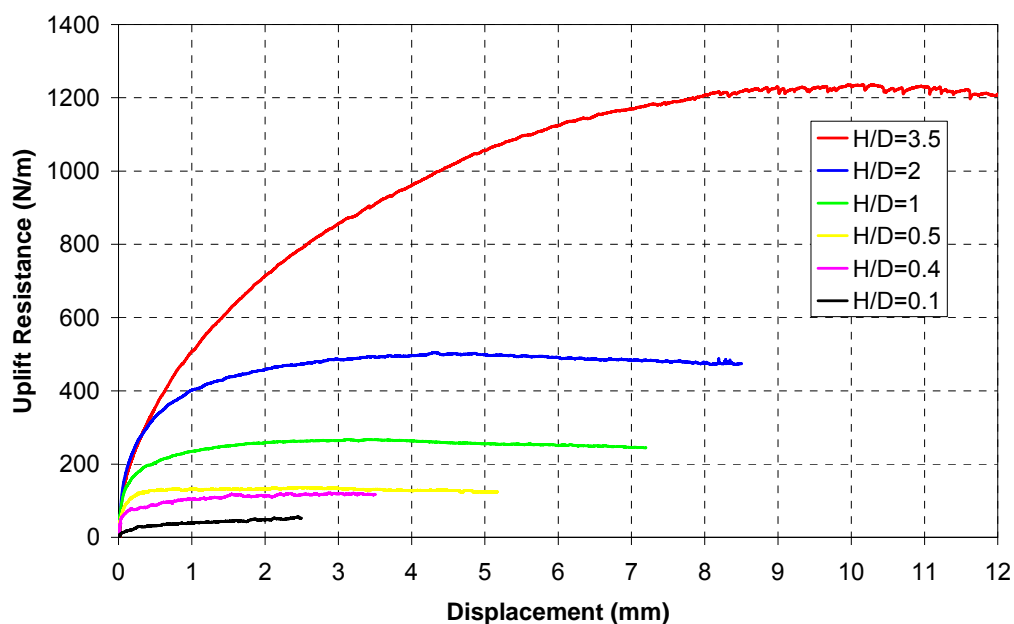


Figure 11 Series 1 Test Results

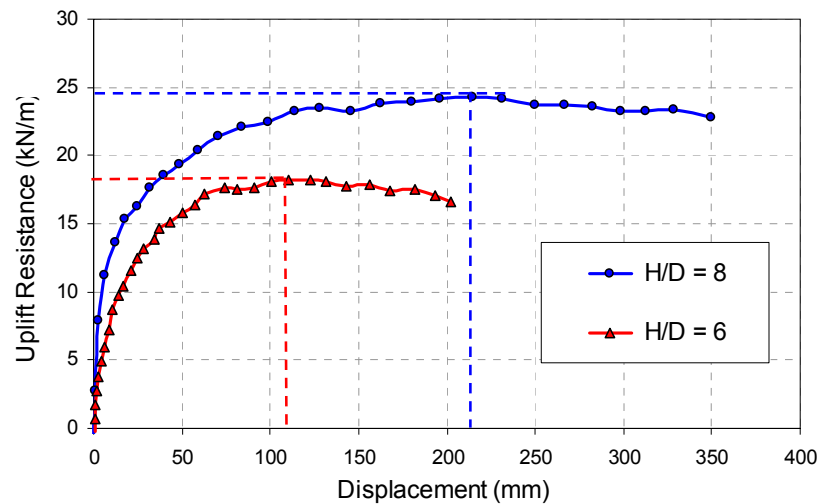


Figure 12 Full Scale Test 9 and 10 Results, (moist loose SAND)

5.2. Uplift Mechanism from Particle Image Velocimetry (PIV)

For Tests No. 1 to 8, the soil displacement field during the uplift event was accurately measured at 5-second intervals, which corresponds to 0.025 mm of upward displacement by the model pipe. This was achieved using the non-contact digital image correlation technique of particle image velocimetry (PIV). The PIV results for H/D=2 test is presented as shear strain plots in Figure 13.

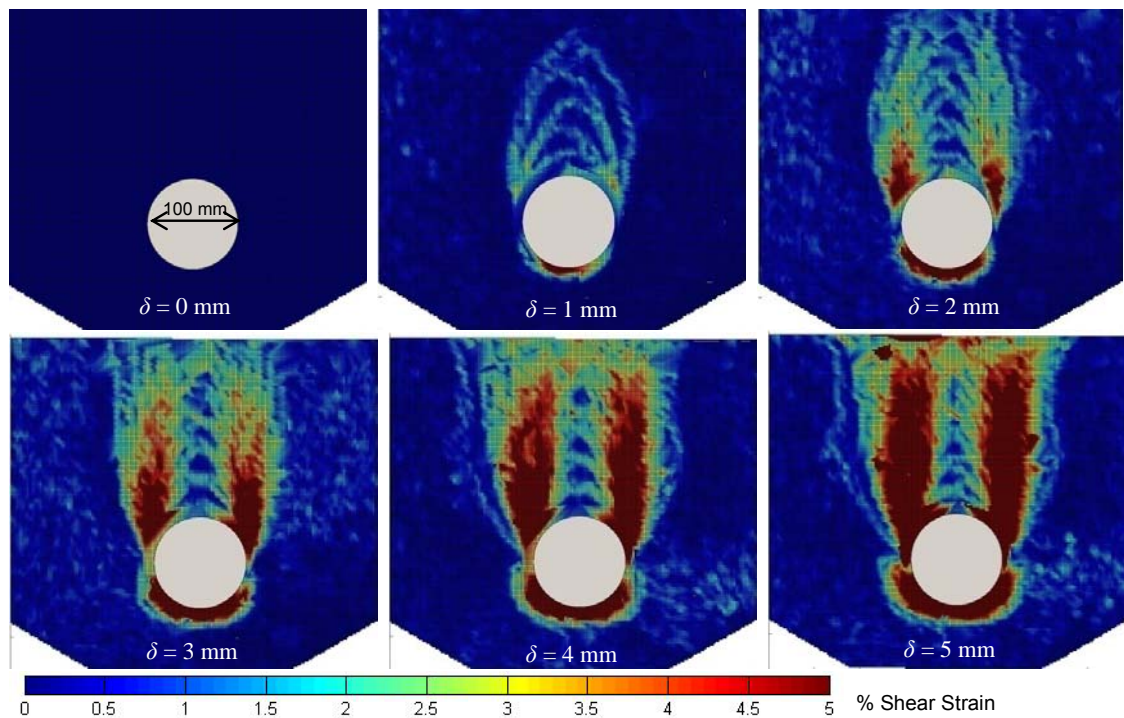


Figure 13 Evolution of total shear strain for Test No. 5, H/D=2, D=100mm

From Figure 13, it is clearly visible that the uplift mechanism in loose sand can be divided into three phases:

1. At very small displacements ($\delta < 1$ mm in this case), thin strands of compression fronts (interpreted as shear bands in total shear strain plots) originate from one side of the pipe crown, fanning out gradually to the other side and swiftly propagating through the backfill soil medium.
2. At small pre-peak displacements ($1 \text{ mm} < \delta < 4.6$ mm in this case), propagation becomes slower and slower and almost comes to a standstill when these compression fronts have rotated over 90° . Subsequent compression fronts start to superimpose on their predecessors. Two cumulated macroscopic shear bands of more than 5% total shear strain originate from both edges of the pipe crown, and start to propagate almost vertically towards the soil surface. R_{peak} is usually reached when this macroscopic shear band just reaches the soil surface.
3. At post-peak displacements ($\delta > 4.6$ mm in this case), the existing mechanism reinforces itself, and the two macroscopic shear bands start to move sideways and widen in a very gradual manner.

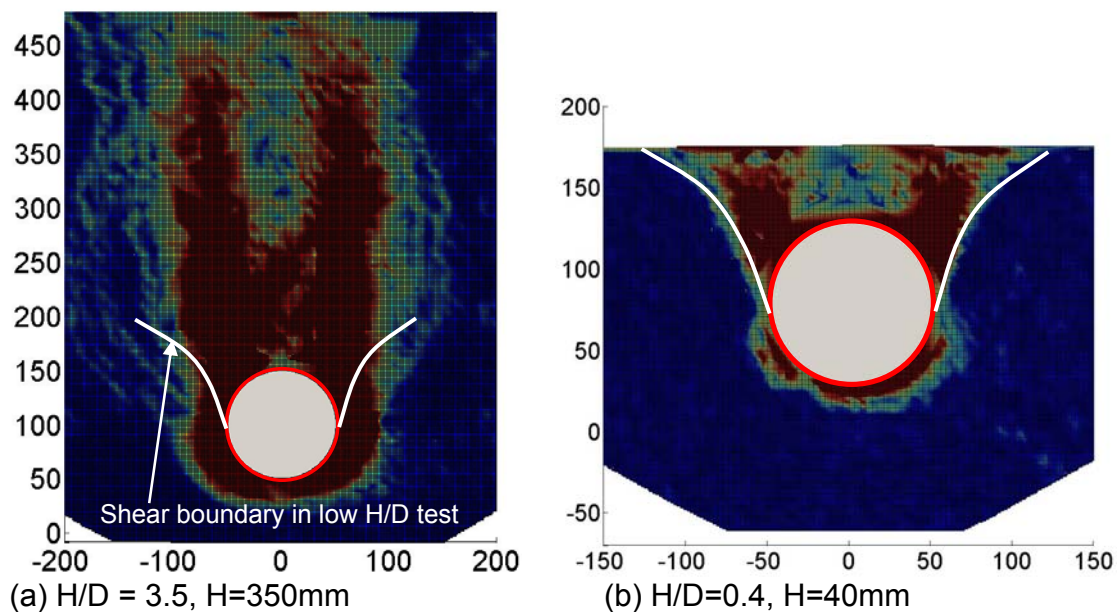


Figure 14 Shear Plots from PIV results

At peak uplift resistance, the centre lines of the two shear bands coincide very well with the two shear planes specified in the Vertical Slip Surface Model. Hence, PIV strain analysis verifies that this model is a good representation of the true uplift deformation mechanism in loose sand at medium H/D ratios. At very low H/D ratios ($H/D \ll 1$), the macroscopic shear bands seem to form a wedge instead of a vertical column at R_{peak} , as illustrated in Figure 14. As a result, more soil volume is being lifted than what is assumed by the Vertical Slip model. This extra contribution from the effective soil weight term is likely to be compensated by the reduction in the shear forces due to reduced normal stress on the two

inclined shear planes compared with the vertical case. Hence the overall deviation from the predicted uplift values using Equation 2 is likely to be small. The uplift resistance of pipeline buried in low cover-diameter ratios is presented in Wang et al. (2010).

6. Discussion

The mobilisation displacement from all the tests are summarised in Figure 15 along with data from published literature. The plot is summarised in δ_f/H for easy comparison with DNV guideline. It is evident from the summarised results that the mobilisation results of higher H/D reported by Trautmann et al. (1985) does not agree with the rest of the data. It should be noted that soil in the “medium” and “dense” tests of Trautmann et al. (1985) was compacted in 100mm layers and hence should be avoided in comparison as rest of the tests are all in loose sands. Furthermore, the Trautmann results does show inconsistency as the mobilisation in loose sand occurs at smaller displacements than that in medium and dense sands. Limitations in the experimental setup and faulty displacement measuring system may have been the cause. This fact is partly acknowledged in the paper as “because a slight displacement was required to seat the connection in the vertical loading system...”, “For tests in medium and dense sand with $H/D=13$, problems with the displacement measuring system prevented accurate determination of Z_f/H ”, where Z_f was mobilisation distance.

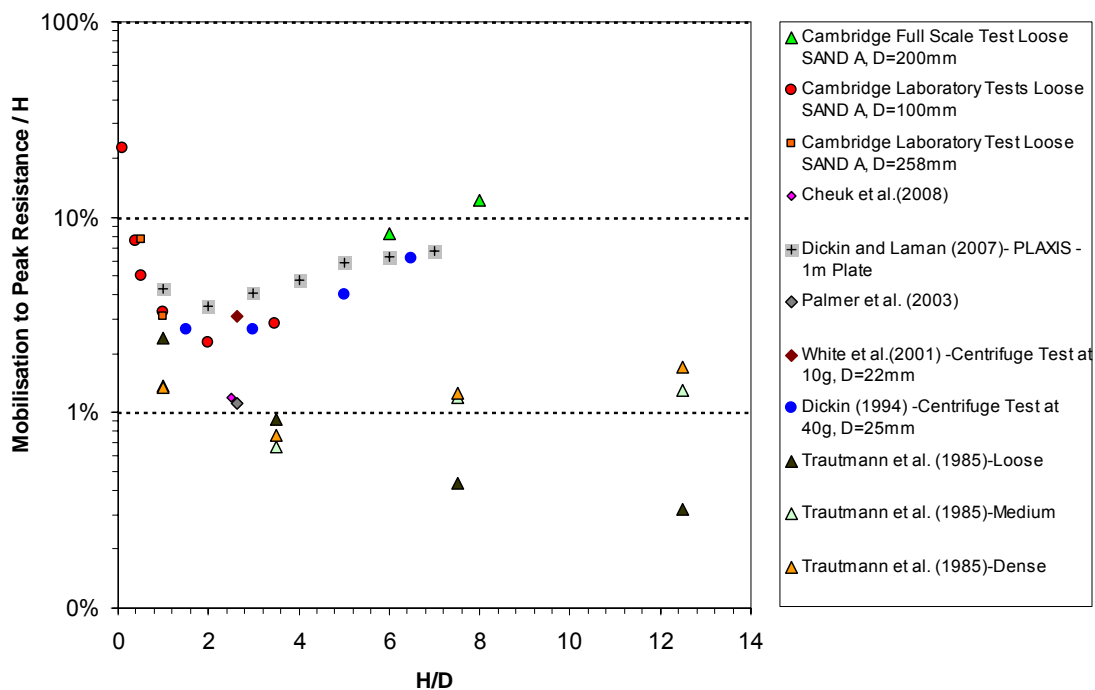


Figure 15 Summary of All Mobilisation Results

Test data and literature data indicates that the mobilisation is a function of H/D. In particular, if Trautmann et al. (1985) is excluded, a good trend in mobilisation can be seen with increasing H/D ratios as shown in Figure 16. Hence, at least up to H/D of 8, a new equation can be proposed that will predict the mobilisation distance in loose sands. This equation is given as,

$$\frac{\delta_f}{D} = 0.02 e^{\left[\frac{1}{2} \frac{H}{D} \right]} \quad \text{Eq. (5)}$$

Note that this equation is base on the available literature which includes dry, moist & submerged sand test data. Hence, any effect of soil saturation (dry, moist & submerged) on mobilisation is not distinguished in this equation

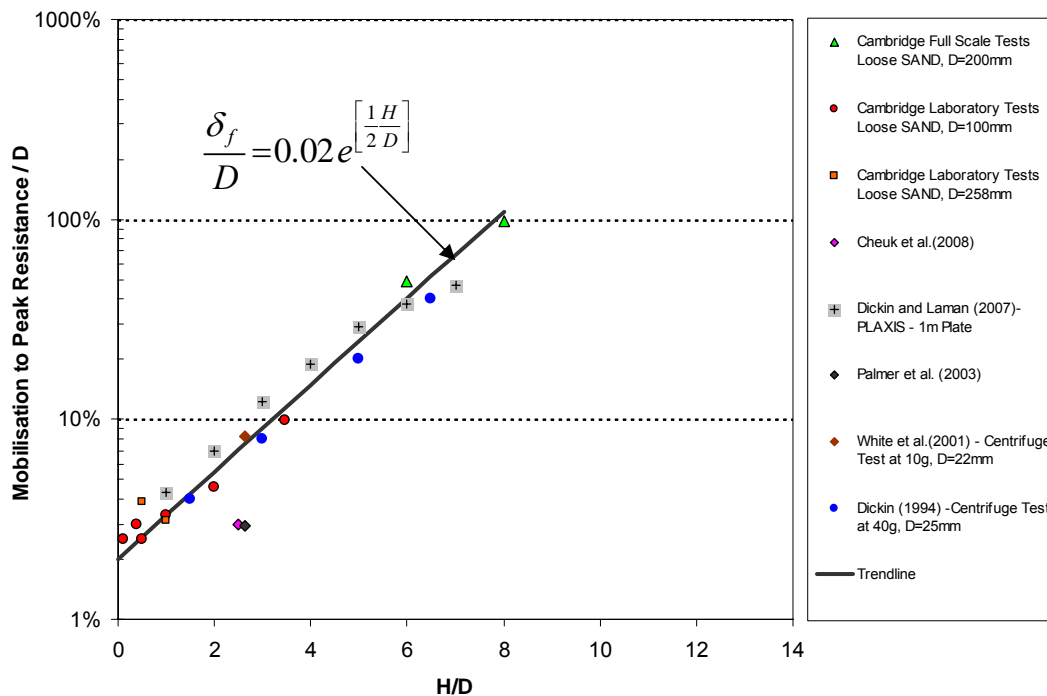


Figure 16 Mobilisation distance vs H/D trendline

It seems as the DNV guideline has followed Trautmann et al. (1985) results alone. The DNV states (Pg 44 of DNV RP F110), "The uplift resistance R_{max} is assumed to be fully mobilised at a vertical uplift displacement δ_f , where δ_f is 0.005-0.01 times the height H . Note that δ_f seems to be independent of the ratio of H/D". The effect of this under-estimation of mobilisation when combined with the use of tri-linear uplift resistance model can lead to unconservative UHB designs. This will be demonstrated in the following sections.

Let us assume a pipe of 0.2m diameter is buried in loose sand with cover $H=1.2m$ (same as in Test 9). If we follow DNV, the mobilisation distance range is

OPT 2010 – 24 & 25 February 2010 – Amsterdam Dr N I Thusyanthan (it206@cantab.net)

6mm-12mm (0.005-0.01H). Let us use a slightly onerous 20mm as the design mobilisation as it is often used in projects. The uplift factor of 0.3 at 20mm will agree with the experimental data. When mobilisation distance of 20mm with $f_p=0.3$ is used with tri-linear uplift resistance model as recommended by DNV, the uplift resistance curves are as shown in Figure 17 (α value of 0.65, 0.75 & 0.85 all are shown). Note that the use of this tri-linear uplift model (any α) with 20mm (or lower as 6mm-12mm) mobilisation leads to stiffer initial response than the true soil resistance. Buckling is a stiffness dominated process, so the most important parameter in determining whether or not a pipeline will buckle is the stiffness of the restraining “spring”. When this is modelled stiffer than in reality, the design is unconservative. An FE assessment will be presented in the next section that will demonstrate this fact.

It is to be noted that when the tri-linear uplift model is applied to the true mobilisation distance (110mm in this case), the initial stiffness is lower than in reality. Thus leading to conservative design.

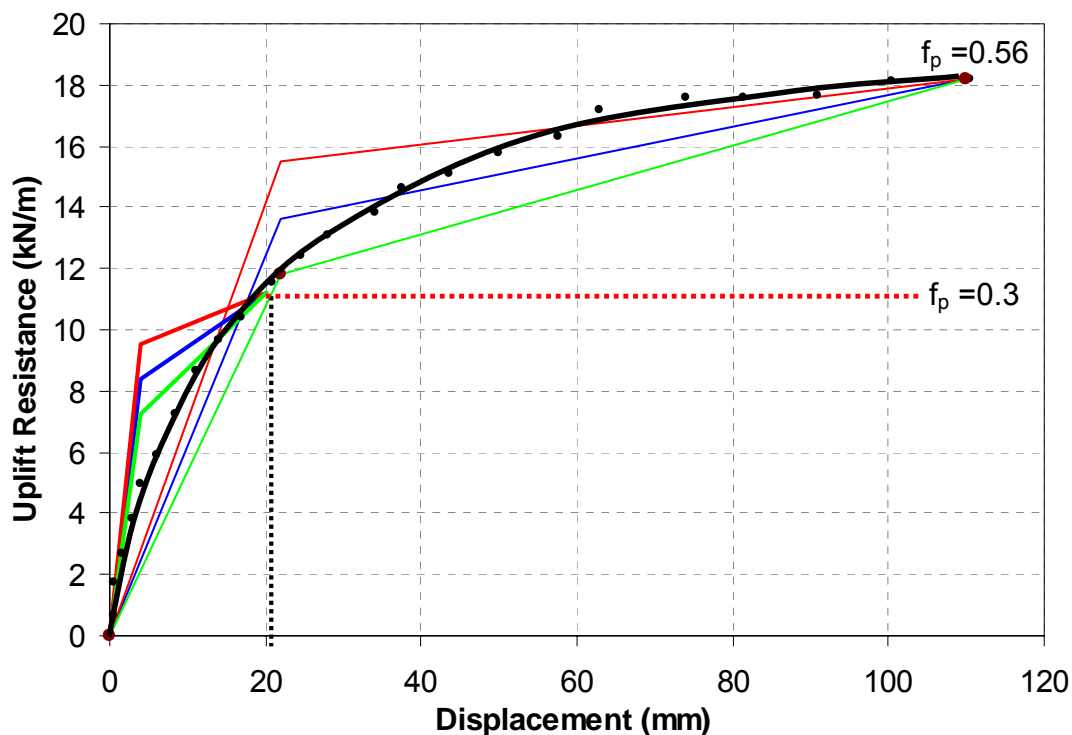


Figure 17 DNV Tri-linear Resistance and true uplift curve for 1.2m SAND cover

It should be noted that downward stiffness of the soil also plays a role in upheaval behaviour buried pipes. This aspect was not investigated in this paper. The FE assessment in the next section assumed stiff downward stiffness in order to eliminate any effect of downward pipe movement on the upheaval behaviour.

7. FE Assessment of Upheaval Buckling

Finite element analyses have been performed using SAGE Profile 2D FE software, utilising six degrees of freedom elastic beam-column element, to investigate the effect of tri-linear uplift resistance model on pipeline upheaval buckling assessment for a fully restraint pipeline section. The four different soil uplift resistance curves that were used in the assessment are shown in Figure 18.

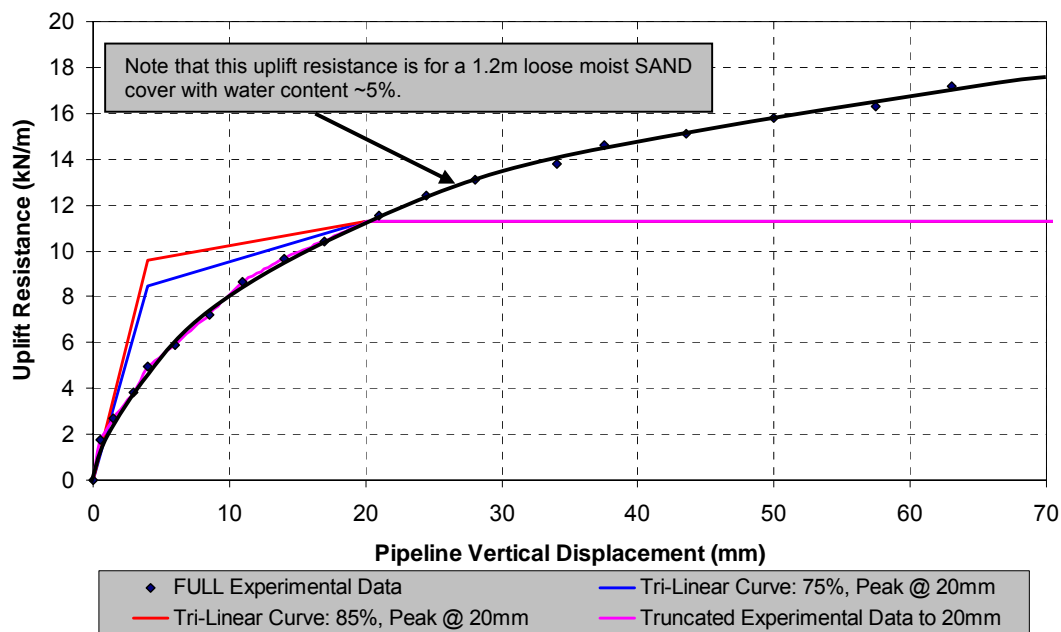


Figure 18 Uplift Resistance from 1.2m sand cover – Pipe D=200mm

A typical short section (1km) of undulated seabed profile was used in the assessment. Four FE runs were carried out, all with same initial pipeline profiles, properties and under same operation conditions (same effective axial forces). The only difference between the analyses was the soil uplift resistance model as shown in Figure 18.

Figure 19 shows the results from the FE assessment. The feature near 60m is seen to mobilise 7mm and 4mm under tri-linear curves (75%, 85%) where as under full uplift resistance, the feature mobilised 44mm. A mobilisation of 61mm is seen when the truncated soil resistance curve was used. For ease of comparison, FE results are superimposed in the soil resistance curves and shown in Figure 20. It is evident that the tri-linear curve results in small pipeline mobilisation and hence leads to the conclusion that no remedial measure is required. However, the use of either the full experimental uplift curve or the truncated experimental uplift curve results in excessive mobilisation which is the reality. The correct conclusion should be to go for remedial measure.

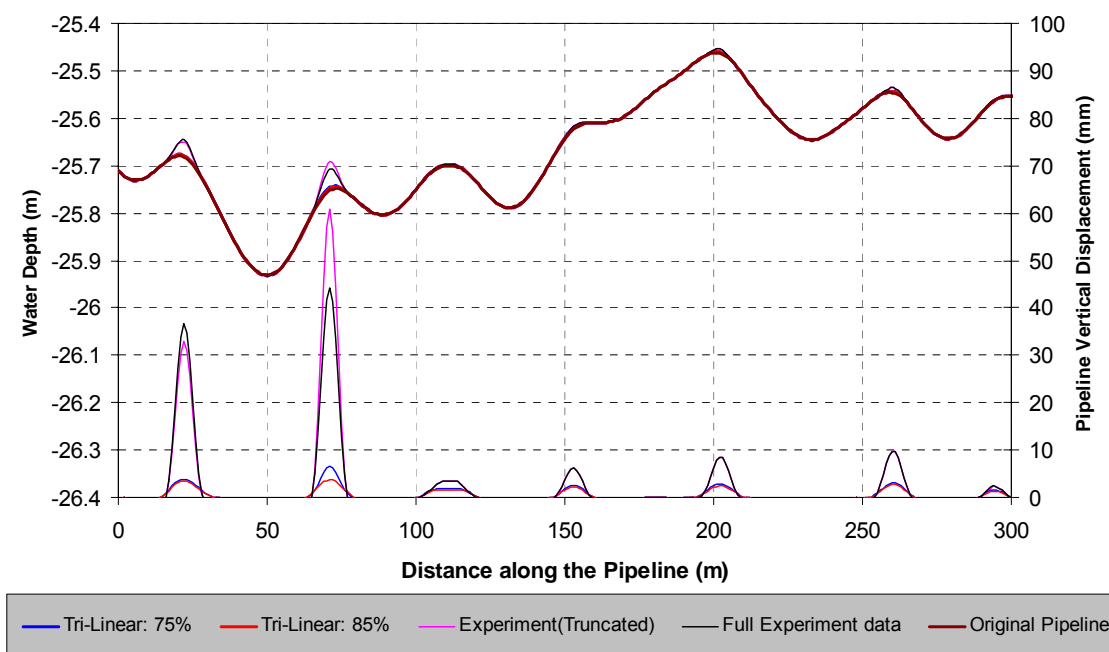


Figure 19 Seabed Profile and Pipeline Deformed Shape – 200mm Pipeline

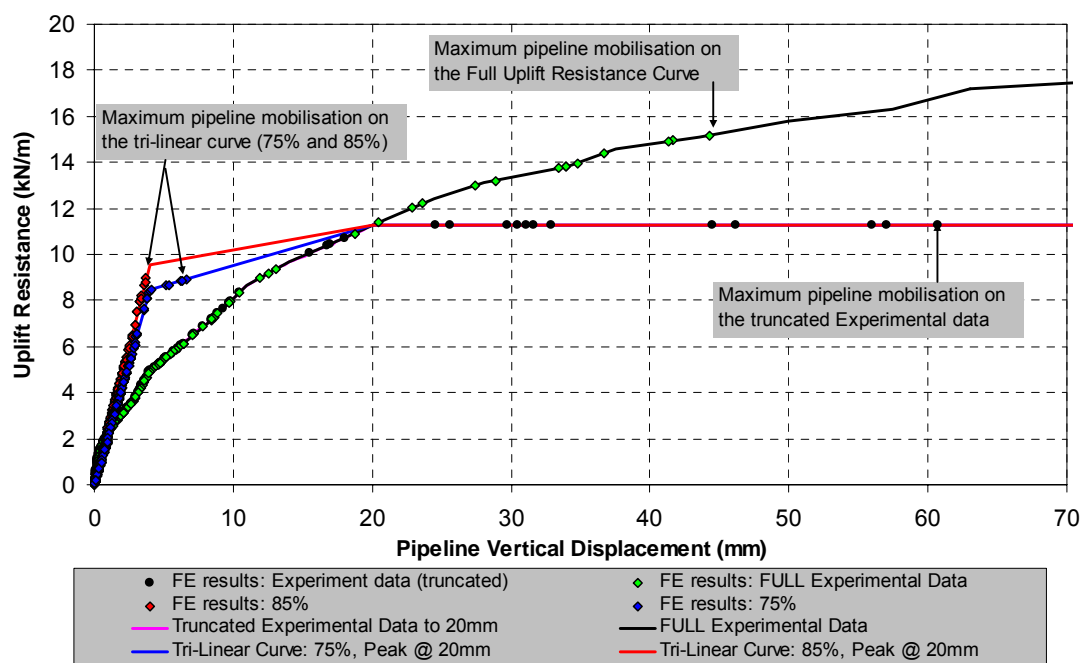


Figure 20 FE Results on Soil Cover Resistance Curves – 200mm Pipeline

It can be concluded that the tri-linear uplift curve of DNV associated with incorrect mobilisation will lead to unconservative final judgement and design conclusions. In light of the above example, if preliminary assessment is required (and no experimental data was available), then bi-linear uplift resistance curve with 20mm mobilisation would be a conservative approach.

8. Conclusions

Upheaval buckling is a common design issue encountered for buried pipelines. Research work presented in this paper highlights the lack in fundamental understanding in pipeline mobilisation required to reach peak uplift resistance.

Current DNV RP F110 recommended practice states that the soil uplift resistance is fully mobilised at a vertical displacement of 0.005-0.01 times H. Experimental data presented in this paper and the data collected from various literature shows that this overly underestimates the true mobilisation distance in loose sands. This underestimation combined with the use of tri-linear soil resistance model recommended by DNV can lead to unconservative pipeline designs. This fact has been demonstrated by FE assessment results.

Based on current experimental results and various data in literature, a new equation is proposed for predicting the peak mobilisation distance in loose sands in terms of H and D. This is as given below,

$$\frac{\delta_f}{D} = 0.02 e^{\left[\frac{1}{2} \frac{H}{D} \right]}$$

Note that any effect of soil saturation (dry, moist & submerged) on mobilisation is not distinguished in this equation. This is being investigated and will be published in a future paper.

A bi-linear uplift curve will yield conservative results if the adopted design mobilisation distance is much smaller than the peak mobilisation (δ_f).

A tri-linear uplift curve should only be used when it is associated with the peak mobilisation distance (δ_f) and peak uplift resistance.

9. Acknowledgement

The authors would like to thank all staff at the Schofield Centre, University of Cambridge for their help and advice throughout the testing program. This research effort has been made possible by the generous financial support provided by Trinity College, University of Cambridge, and KW Ltd.

10. References

- Baumgard, A.J. (2000). Monotonic and cyclic soil response to upheaval buckling in offshore buried pipelines. *PhD Thesis*. University of Cambridge.
- Bransby, M.F. and Ireland, J. (2009). Rate effects during pipeline upheaval buckling in sand. *Geotechnical Engineering* **162**: 247-256.
- Cheuk C. Y., White D. J. and Bolton M. D. (2008), Uplift Mechanisms of Pipes Buried in Sand, *Journal of Geotechnical and Geoenvironmental Engineering*, Vol. 134(2), 154-163.
- Croll, J.G.A. (1997). A simplified model of upheaval thermal buckling of subsea pipelines. *Thin-Walled Structures* **29** (1-4): 59-78.
- Dickin, E.A. (1994). Uplift resistance of buried pipelines in sand. *Soils and Foundations* **34** (2): 41-48.
- Dickin, E.A. and Laman, M. Uplift response of strip anchors in cohesionless soil. *Advances in Engineering Software* **38** (8-9): 618-625.
- DNV-RP-F110, Global buckling of submarine pipelines – structural design due to high temperature / high pressure. *Det Norske Veritas*, Norway, 2007.
- Palmer, A.C., Ellinas C.P., Richards, D.M., and Guijt, J. (1990). Design of submarine pipelines against upheaval buckling. *Proc. Offshore Technology Conf., Houston*, OTC 6335: 551-560.
- Palmer, A.C. White, D.J., Baumgard, A.J., Bolton, M.D., Barefoot, A.J. Finch, M., Powell, T., Faranski, A.S., Baldry, J.A.S. (2003). Uplift resistance of buried submarine pipelines: comparison between centrifuge modeling and full-scale tests. *Géotechnique* **53** (10): 877–883
- Pedersen, P.T. & Jensen, J.J. (1988). Upheaval creep of buried pipelines with initial imperfections. *Marine Structures* **1**:11-22, 1988.
- Schaminée, P.E.L., Zorn, N.F., and Schotman, G.J.M. (1990). Soil response for pipeline upheaval buckling analysis: Full-scale laboratory tests and modelling. *Offshore Technology Conference*, Houston, OTC 6486
- Timoshenko, S. and Goodier, J. N. (1934). *Theory of Elasticity*. McGraw-Hill Book Company.
- Trautman, C.H., O'Rourke, T.D., and Kulhawy, F.H. (1985). Uplift force-displacement response of buried pipe. *ASCE Journal of Geotechnical Eng. Division* **111** (9): 1061-1075.
- Thusyanthan, N.I., Ganesan S. A & Bolton M.D. and Peter Allan (2008), *Upheaval buckling resistance of pipelines buried in clayey backfill*, Proceeding of ISOPE 2008, The Eighteenth (2008) International Offshore and Polar Engineering Conference, Vancouver, Canada
- Vesic, A.S. (1971). Breakout resistance of objects embedded in ocean bottom. *ASCE Journal of the Soil Mechanics and Foundation Division*. **97** (9): 1183-1205.
- Wang, J., Haigh, S.K., and Thusyanthan, N.I. (2009). Uplift resistance of buried pipelines in blocky clay backfill. *Proc. International Offshore (Ocean) and Polar Engineering Conference*. ISOPE 2009 TPC 564.
- Wang, J., Haigh, S.K., and Thusyanthan, N.I. (2010). Uplift resistance design of shallowly buried pipelines. *ASCE Pipelines Journal* (currently being drafted).
- White, D.J., Barefoot, A.J., Bolton, M.D. (2001). Centrifuge modelling of upheaval buckling in sand. *International Journal of Physical Modelling in Geotechnics*, **2** (1):19-28.
- White, D. J., Take, W. A. & Bolton, M. D. (2003). Soil deformation measurement using particle image velocimetry (PIV) and photogrammetry. *Géotechnique*, **53** (7): 619–631.